Influence of Mass-Transfer Limitations on Carbon Isotope Fractionation During Microbial Dechlorination of Trichloroethene

Christoph Aeppli°‡, Michael Berg°, Olaf A. Cirpka°‡, Christof Holliger§,

*René P. Schwarzenbach#, and Thomas B. Hofstetter# **

° Eawag, Swiss Federal Institute of Aquatic Science and Technology, 8600 Dübendorf, Switzerland,

§Laboratoire de biotechnologie environnementale, EPF Lausanne, 1015 Lausanne, Switzerland,

#Institute of Biogeochemistry and Pollutant Dynamics (IBP), ETH Zurich, 8902 Zurich, Switzerland

*Corresponding author phone: +41 44 632 83 28

e-mail: thomas.hofstetter@env.ethz.ch

‡ current addresses: CA: Department of Applied Environmental Science (ITM), Stockholm University, Sweden; OAC: University of Tübingen, Center for Applied Geoscience (ZAG), Tübingen, Germany

Abstract

Mass transfer of organic contaminants from non-aqueous phase liquids to the aqueous phase can significantly modulate the observable carbon isotope fractionation behavior associated with contaminant transformation. We evaluated the effects of kinetic inter-phase mass transfer between tetradecane and water on the observable ^{13}C enrichment factor, ε_{obs}, pertinent to the reductive dechlorination of trichloroethene (TCE) by *Sulfurospirillum sp*. in laboratory batch model systems containing organic, aqueous and gaseous phases. We propose a conceptual model, which includes the kinetics of tetradecane-water and gas-water mass transfer, microbial growth and isotope-sensitive parameters describing dehalorespiration, for quantifying variable ^{13}C enrichment factors. While the C isotope fractionation of TCE reduction to *cis*-dichloroethene (cDCE) in the absence of phase-transfer effects can be characterized by a constant ε-value of -18.8±0.6‰, mass-transfer limitations impede describing this process with a constant enrichment factor typically used in Rayleigh equations. Owing to the masking of kinetic isotope effects by the transfer of TCE from tetradecane to the aqueous phase, ε_{obs}-values gradually changed from -18.4‰ to -5.9‰. Such variations may complicate the interpretation of compound-specific isotope analysis in the assessment of chloroethene biodegradation in field applications.

Introduction

Tetrachloroethene (perchloroethene, PCE) and trichloroethene (TCE) are among the most widespread (eco-)toxic soil and groundwater contaminants. These compounds persist for decades in the presence of oxygen but can be transformed under anoxic conditions by specialized microorganisms in respiratory or cometabolic processes *(1)*. Depending on the bacterial community and the prevailing environmental conditions, sequential reductive dechlorination *via* dichloroethenes (DCE) and vinyl chloride (VC) can proceed to the benign products ethene and ethane thus offering a viable bioremediation option for numerous contaminated sites. For the assessment and monitoring of chloroethene attenuation as well as for mitigating possible drinking water contamination in practice, however, a reliable identification and quantification of PCE and TCE biotransformation is essential. Because of the inherent difficulty to differentiate between contaminant reactions and non-degradative processes such as dilution and sorption on the basis of concentration measurements, compound-specific isotope analysis (CSIA) has increasingly been applied to assess *in-situ* degradation of pollutants *(2, 3* and references therein*)*. Owing to a preferential transformation of chloroethenes containing light stable carbon and chlorine isotopes (i.e., ^{12}C vs. ^{13}C, ^{35}Cl vs. ^{37}Cl), it has been suggested quantifying the extent of biotransformation *B* on the basis of a contaminant's isotopic fractionation, that is changes of isotope signatures, $\delta^h E$ (*(4-8)*, eq. 1):

$$B = 1 - \frac{C}{C_0} = 1 - \left(\frac{\delta^h E + 1000‰}{\delta^h E_0 + 1000‰} \right)^{\frac{1000‰}{\varepsilon_E}} \qquad (1)$$

where C/C_0 is the fraction of remaining reactant and $\delta^h E$ stands for the $\delta^{13}C$ or $\delta^{37}Cl$ values of the chloroethenes in per mil, for example along a contaminant plume (subscript "0" is its initial value), and ε_E is the isotope enrichment factor of C or Cl pertinent to a specific reaction. Even though aquifers exhibit considerable heterogeneity, the Rayleigh equation (eq. 1) has been shown to be applicable to field situations *(9)*. However, a rather wide range of C isotope enrichment factors has been reported for the reduction of PCE, TCE, DCE and VC by different dehalogenating bacteria or under varying experimental conditions *(10-13)* thus making a quantitative interpretation of isotope signatures less

reliable. Such variations in the isotope enrichment behavior can arise from competing reaction mechanisms and/or reaction kinetics such as different rate-limiting steps in dehalogenating enzymes or a masking of isotopic reactions by transport processes (e.g., to active sites, across membranes etc.). Competing reaction mechanisms can be identified with multi-element isotope analyses (e.g., *(11, 14-16)*), especially since on-line methods for the CSIA of Cl isotopes in chloroethenes are becoming available *(11, 17)*. In contrast, much less is known about the variations of bulk enrichment factors due to masking of isotope fractionation by mass-transfer limitations and/or bioavailability constraints *(18)*.

In fact, the mass transfer of PCE or TCE from non-aqueous phase liquids (NAPLs), which act as source zones of contamination plumes at field sites and emit pollutants for decades, are likely to lead to variations of observable isotope fractionation behavior (i.e., ε_E-values) during chloroethene biodegradation. NAPL dissolution rates are highly variable in aquifers and depend on groundwater velocity, NAPL architecture, microbial activity, among other factors *(19, 20)*, and can even limit the microbial chloroethene reduction altogether *(21)*. Thus, one can envision a regime of fast NAPL dissolution and low microbial activity, in which mass transfer hardly affects the observable isotope fractionation. In such a situation the bulk isotope enrichment factors can be expected to take on values that are typical for a given type of microbes and transformation mechanism *(22)*. In contrast, slow NAPL dissolution coupled with high microbial dechlorination activity likely leads to vanishing isotope effects. In the transition between these two regimes, isotope enrichment factors are not necessarily constant and an evaluation of chloroethene isotope signatures may not follow the Rayleigh equation (eq. 1).

The goal of this work was to quantify the effects of inter-phase mass-transfer limitations, as they might occur during NAPL dissolution, on the observable carbon isotope fractionation during dehalorespiration of chloroethenes. To this end, we developed a conceptual model for evaluating carbon isotope fractionation during the microbial reduction of TCE to cDCE in laboratory batch systems *(23-25)* containing anaerobic dehalorespiring bacteria of the genus S*ulfurospirillum* with and without

transport limitations caused by TCE inter-phase mass transfer. A non-aqueous phase liquid was mimicked using tetradecane as organic phase rather than pure phase TCE given that the latter can potentially poison the bacteria and that TCE often occurs as a co-contaminant in light and dense NAPLs.

Materials and Methods

Chemicals. *n*-Hexadecane, *n*-tetradecane, tetrachloroethene (PCE), trichloroethene (TCE), *cis*-1,2-dichloroethene (cDCE), *trans*-1,2-dichloroethene (tDCE), 1,1-dichloroethene (11DCE), deuterated methyl *tert*-butyl ether (MTBE-d_3) and deuterated chloroform (CF-d) were purchased from Sigma-Aldrich in the highest available purity.

Cultivation of *Sulfurospirillum sp.* A highly enriched sediment-free cultures containing one pre-dominant gram-negative bacterium belonging to the sub-group of ε-proteobacteria and affiliating with the genus *Sulfurospirillum* (16S mRNA gene analysis) was used as inoculum (see Supporting Information (SI) for more details). Pre-cultures were cultivated anaerobically in 118 mL Viton®-stopper-sealed glass serum flasks. The incubation flasks contained 50 mL bicarbonate-phosphate-buffered minimum salt medium *(26)* without yeast extract. Acetate was added as carbon source (2 mM) and H_2 as electron donor (headspace containing H_2/CO_2 = 80/20 v:v at $1.5 \cdot 10^5$ Pa). Cultures were incubated in the dark at 30°C without shaking. PCE, added in a 5 mL *n*-hexadecane solution (100 mM PCE), was sequentially dechlorinated *via* TCE to cDCE (95%), tDCE (4.4%) and 11DCE (0.6%) within one week. Pre-cultures were used for TCE biodegradation experiments (see next section) after >30 sequential transfers of cultures with 1 mL inoculum from preceding cultures that were in the late exponential growth phase.

Microbial Dechlorination of TCE. All experiments were conducted in duplicates in 118 mL Viton®-stopper-sealed glass serum flasks. Three-phase systems (50 mL anaerobic minimum salt medium with 1 mM acetate, 15 mL tetradecane containing 50 mM TCE, headspace H_2/CO_2 80/20 v:v) were inoculated with 5 mL pre-culture medium in the late exponential phase that contained exclusively

DCE isomers from PCE hydrogenolysis as confirmed by GC/FID-analysis of headspace samples. All batch cultures were incubated on an orbital shaker (60 rpm) in the dark at 25 °C. The identical experimental setup was used for a two-phase system (gas and aqueous phase) where TCE was amended by adding 5 mL TCE-saturated medium (8.3 mM TCE) instead of a TCE tetradecane solution. Reactors were inoculated with 1 mL pre-culture medium at 25 °C in the dark on an orbital shaker at 160 rpm. At regular time intervals, samples were withdrawn from the aqueous phase (2.5-4.5 mL) and from the tetradecane phase (400 μL) using gas-tight glass syringes (Hamilton, Bonaduz, Switzerland) for the analyses of TCE and cDCE concentrations and ^{13}C signatures. Furthermore, chloride, acetate, and cell densities were measured in aqueous samples. Reactions in the aqueous samples were stopped by dilution with oxic water (1:40 to 1:200, depending on the concentration of TCE).

Analytical Methods. For concentration measurement of TCE and DCE isomers, aqueous samples were diluted (1:50) and spiked with internal standards (MTBE-d_3 and $CDCl_3$) for analysis by direct aqueous injection (DAI) coupled to GC/MS *(27)*. Concentration of TCE and cDCE in the organic phase were measured by GC/FID according to the methods given in the Supporting Information (SI).

Carbon isotope analysis of TCE and cDCE of aqueous and organic samples was performed with a gas chromatograph coupled to an isotope ratio mass spectrometer *via* a combustion interface (GC Combustion III, Thermo Scientific) maintained at 940°C. For the aqueous samples, a slightly modified purge & trap-GC/C/IRMS procedure described previously *(28)* was applied (5 minutes purge time, no cryogenic interface). The GC was equipped with a 60 m Rtx-VMS column (0.32 mm I.D., 1.8 µm film; Restek Corp.) and the temperature program was 40°C (5 min), ramped to 100°C at 15°C/min, then to 200 °C at 30 °C/min, hold 4 min. The samples from the organic phase were injected on-column in the GC/C/IRMS system (see SI for details). All isotopic signatures are reported relative to the international standard Vienna PeeDee Belemnite (VPDB) in the delta notation as $\delta^{13}C$. Before each sample measurement, the IRMS was internally calibrated with reference CO_2 gas. The accuracy of isotope ratio measurements was ensured by analyzing standard solutions containing TCE and cDCE with known

isotopic composition in the same matrix and concentration range every ten measurements. All samples were measured in duplicates and uncertainties of $\delta^{13}C$-values of standards and replicates were below ±0.5‰.

Chloride and acetate concentrations were quantified by ion chromatography and reversed-phase HPLC, respectively, according to methods described in the Supporting Information (SI). Cell densities were determined by flow-cytometric enumeration (in 3.5% formaldehyde solution) following procedures described in reference *(29)*.

Data Evaluation and Mathematical Model. A schematic representation of the experimental system made up of aqueous (*aq*), organic (*org*), and gaseous (*gas*) phases is illustrated in Figure 1. Isotopologues of TCE and cDCE containing only ^{12}C atoms (^{12}TCE, ^{12}cDCE) and one ^{13}C and one ^{12}C atom (^{13}TCE, ^{13}cDCE) were treated as independent components. The isotopologues containing only ^{13}C are negligible at natural abundance carbon isotopes distribution. Whereas TCE, cDCE, and molecular hydrogen (H_2) were present in the aqueous, organic, and gaseous phases, dechlorinating bacteria existed exclusively in the aqueous phase. Two processes were assumed to determine species and isotopologue concentrations in the three-phase experimental system, that is hydrogenolysis of TCE to cDCE *(23)* and kinetic inter-phase mass transfer of TCE, cDCE, and H_2. Microbial transformation rates of the ^{i}TCE isotopologues, ^{i}r (superscript i denotes rates of ^{12}TCE and ^{13}TCE reduction, respectively) were modeled by dual Monod kinetics (eq. 2) and included the competitive inhibition of the isotopologues. Note that competition by ^{13}TCE isotopologues can be neglected.

$$ {}^{i}r = \frac{{}^{i}k}{{}^{i}K_{M,TCE}} \cdot \frac{[{}^{i}TCE]_{aq}}{\left(1 + [{}^{12}TCE]_{aq} / {}^{12}K_{M,TCE}\right)} \cdot \frac{[H_2]_{aq}}{K_{M,H_2} + [H_2]_{aq}} \cdot X \qquad (2) $$

where ^{i}k is the maximum specific reaction rate per TCE isotopologues and biomass (^{12}k and ^{13}k, unit μmol h^{-1}·$cell^{-1}$), $K_{M,TCE}$ represents the Monod constant of TCE assumed identical for both isotopologues (unit μmol·L^{-1}), $[^{i}TCE]_{aq}$ and $[H_2]_{aq}$ are the aqueous concentration of ^{i}TCE and H_2, $K_{M,H2}$ is the Monod constants for H_2, and X is the biomass concentration (in cells·L^{-1}). Inter-phase mass transfer was

described by a linear-driving-force model *(30)* leading to the following differential equations (eqs. 3-6) for the aqueous concentration of ^{i}TCE, ^{i}cDCE, H_2 (in μmol·L^{-1}), and biomass concentration *X*:

$$\frac{d[^{i}TCE]_{aq}}{dt} = -^{i}r + \kappa_{TCE}^{org-aq} \cdot a_0^{aq} \cdot \left([^{i}TCE]_{aq}^{eq} - [^{i}TCE]_{aq}\right) \quad (3)$$

$$\frac{d[^{i}cDCE]_{aq}}{dt} = +^{i}r + \kappa_{cDCE}^{org-aq} \cdot a_0^{aq} \cdot \left([^{i}cDCE]_{aq}^{eq} - [^{i}cDCE]_{aq}\right) \quad (4)$$

$$\frac{d[H_2]_{aq}}{dt} = -(^{12}r + ^{13}r) + \kappa_{H_2}^{org-aq} \cdot a_0^{aq} \cdot \left([H_2]_{aq}^{eq} - [H_2]_{aq}\right) \quad (5)$$

$$\frac{dX}{dt} = Y \cdot (^{12}r + ^{13}r) \quad (6)$$

where κ_{TCE}^{org-aq} and κ_{cDCE}^{org-aq} are the organic (i.e., tetradecane) to aqueous phase mass-transfer coefficients of TCE and cDCE (in cm·h^{-1}), a_0^{aq} is the interface area per unit volume of the aqueous phase (cm^{-1}), $[^{i}TCE]_{aq}^{eq}$, $[^{i}cDCE]_{aq}^{eq}$, and $[H_2]_{aq}^{eq}$ are the equilibrium concentrations of the chloroethene isotopologues and hydrogen in the aqueous phase with respect to the organic phase. *Y* stands for a yield factor (cells·μmol^{-1}) and describes the increase in microbial biomass per unit of TCE transformed. Because the aqueous phase was not in direct contact with the gas phase in the three-phase system, no mass transfer between these two phases was included in the model. Mass transfer between the organic and gaseous phases was calculated as shown in eqs. 7-8 where *j* stands for the concentrations of chloroethene isotopologues (^{i}TCE, ^{i}cDCE) and H_2.

$$\frac{d[j]_{org}}{dt} = -\kappa_j^{org-aq} \cdot a_0^{org} \cdot \left([j]_{aq}^{eq} - [j]_{aq}\right) - \kappa_j^{org-gas} \cdot a_0^{org} \cdot \left([j]_{gas}^{eq} - [j]_{gas}\right) \quad (7)$$

$$\frac{d[j]_{gas}}{dt} = -\kappa_j^{org-gas} \cdot a_0^{gas} \cdot \left([j]_{gas}^{eq} - [j]_{gas}\right) \quad (8)$$

To evaluate experimental data from the two-phase system, the organic to aqueous phase mass transfer was replaced by the one between gas and aqueous phase (κ^{org-aq} for TCE and cDCE were replaced by κ^{gas-aq} in eqs. 3-5, 8) while equation 7 became obsolete.

The system of differential equations 3-8 was solved numerically. To avoid negative parameter values (except for epsilon) the logarithms of all model parameters were fit to experimental data minimizing the sum of squared residuals of TCE, cDCE, and *Sulfurospirillum sp*. cell concentration as well as the δ^{13}C-values of TCE and cDCE, weighted by the uncertainty of the measurements (see SI for squared residuals and MATLAB codes).

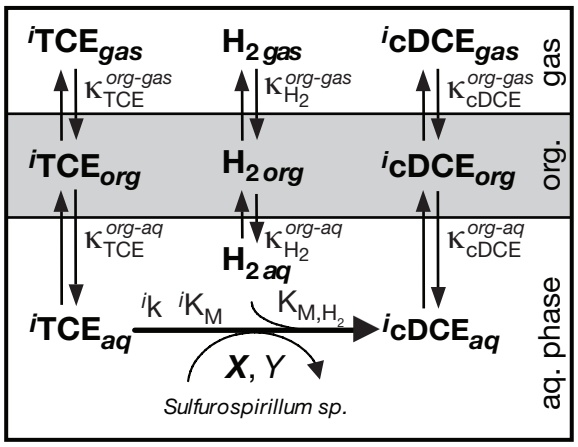

Figure 1: Processes in the three-phase batch system. Horizontal arrow: Aqueous ^{12}TCE and ^{13}TCE are microbially transformed to ^{12}cDCE and ^{13}cDCE, coupled to growth of *Sulfurospirillum* sp biomass *X* with yield factor *Y* and consumption of H_2. Different rate constants ^{i}k for ^{i}TCE isotopologues (i=12, 13) lead to isotopic fractionation. K_M and $K_{M,H2}$ are the Monod-constants for TCE and H_2, respectively. Vertical arrows: The kinetic inter-phase mass transfer of compound j (j=^{i}TCE, ^{i}cDCE and H_2) between the adjacent phases x and y is driven by the concentration difference times a mass-transfer coefficient κ_j^{x-y}.

Isotope Fractionation. The isotope fractionation in enzymatic reactions is given by the fractionation factor α, which corresponds to the ratio of reaction rates for heavy and light TCE isotopologues and can also be expressed by each isotopologues' maximum specific reaction rate divided by the corresponding Monod constant. In the absence of mass-transfer limitations, a reference fractionation factor, α_{ref}, for TCE hydrogenolysis is given in eq. 9 *(31)*.

190 $$\alpha_{ref} = \frac{^{13}k\,/^{13}K_M}{^{12}k\,/^{12}K_M} = \frac{^{13}r}{^{12}r} \cdot \frac{[^{12}TCE]_{aq}}{[^{13}TCE]_{aq}} \quad (9)$$

191 To account for a modulation of α_{ref} by mass-transfer effects between the organic and aqueous phases
192 in the three-phase systems, an observable C isotope fractionation factor in the aqueous phase, α_{obs}, was
193 defined (eq. 10). α_{obs} includes a possible decrease of the apparent rate of TCE isotopologue
194 hydrogenolysis, ^{i}r, owing to a limited mass transfer of TCE from the organic to the aqueous phase
195 ($\kappa_{TCE}^{org-aq} \cdot a_0^{aq} \cdot \left([^{i}TCE]_{aq}^{eq} - [^{i}TCE]_{aq}\right)$). As will be shown below, the isotope fractionation associated with
196 mass transfer is negligible.

197 $$\alpha_{obs} = \frac{\frac{d[^{13}TCE]_{aq}}{dt}}{\frac{d[^{12}TCE]_{aq}}{dt}} \cdot \frac{[^{12}TCE]_{aq}}{[^{13}TCE]_{aq}} = \frac{^{13}r - \kappa_{TCE}^{org-aq} \cdot a_0^{aq} \cdot \left([^{13}TCE]_{aq}^{eq} - [^{13}TCE]_{aq}\right)}{^{12}r - \kappa_{TCE}^{org-aq} \cdot a_0^{aq} \cdot \left([^{12}TCE]_{aq}^{eq} - [^{12}TCE]_{aq}\right)} \cdot \frac{[^{12}TCE]_{aq}}{[^{13}TCE]_{aq}} \quad (10)$$

198 **Determination of Aqueous – Organic Phase Mass-Transfer Rates.** TCE and cDCE mass-transfer
199 coefficients between the aqueous and *n*-tetradecane phases were determined using a linear-driving force
200 model *(30)* for 60 rpm shaking velocities in a sterile three-phase batch system containing 50 mL
201 medium, 15 mL tetradecane, and 53 mL headspace. After the addition of TCE or cDCE to the aqueous
202 phase, the decrease in aqueous concentrations of TCE and cDCE was monitored with time. The
203 following rate coefficients of mass transfer were fit with the mathematical model introduced above:
204 1.8±0.3 cm·h^{-1} for κ_{TCE}^{org-aq} and 2.0±0.8 cm·h^{-1} for κ_{cDCE}^{org-aq}. No significant isotopic shifts of TCE and
205 cDCE ($\Delta\delta^{13}C$ <0.5 ‰) were observed in the aqueous phase during the mass-transfer experiments. This
206 observation suggests that the chloroethene mass transfer between medium and tetradecane was not
207 isotope-sensitive (see Figure S1).

208 **Results and Discussion**

Reduction of TCE to cDCE in aqueous solution. The hydrogenolysis of 0.4 mM TCE to cDCE within 60 hours in aqueous-gaseous phase batch reactors by *Sulfurosprillum sp*. is shown in Figure 2A. Aqueous cDCE concentration slightly exceeded the initial aqueous concentration of TCE owing to the more pronounced tendency of TCE to partition into the gas-phase (dimensionless $K_{air\text{-}water}$ of cDCE equals 0.16 compared 0.40 for TCE *(32)*). A mass balance calculation including chloroethenes in the gas and aqueous phase revealed stoichiometric transformation of 30 µmol TCE to cDCE (Figure S2). The corresponding ^{13}C enrichment in the remaining TCE is illustrated in Figure 2E. $\delta^{13}C$-trends of cDCE did not show the typical initial depletion in ^{13}C compared to the $\delta^{13}C$-values of TCE due to the transfer of approximately 2 μmol cDCE from the pre-culture with the inoculum. After 40 hours, cDCE originated mainly from the isotopically depleted cDCE of the ongoing hydrogenolysis and the final $\delta^{13}C$-value of cDCE matched the original $\delta^{13}C$ of TCE at the end of the reaction.

Influence of Tetradecane-Water Partitioning of Chloroethenes on Kinetics and Isotope Fractionation During TCE Respiration. The concentration trends of TCE and cDCE in the aqueous phase in the presence of tetradecane (three-phase system, Figure 2B and C, 50 mM initial TCE concentration in the organic phase) were comparable to those without organic phase. Owing to the different tetradecane-water partitioning constants of TCE and cDCE ($K_{tetradecane\text{-}water}$ of TCE equals 430 compared to 40 for cDCE, see SI), the final aqueous cDCE concentration was about one order of magnitude higher than the initial aqueous TCE concentration. This aqueous TCE concentration dropped within 48 h to a level of 20-30 μmol·L^{-1} due to limited TCE supply from the organic phase while the cDCE concentration increased constantly during up to 120 h. In the tetradecane phase, the concentration trends were similar to those in the aqueous phase (Figure 2C). A mass balance calculation (Figure 2D) revealed a near stoichiometric reduction of 770 μmol of TCE to 690 μmol cDCE, which is supported by the detection of 750 μmol of aqueous Cl^-. In contrast to the chloroethene concentration dynamics, the $\delta^{13}C$ evolution of TCE in the three-phase system exhibited less pronounced carbon isotope enrichment, especially in the organic phase (Figures 2F and G). In analogy to the two-phase system, trends of cDCE-

234 $\delta^{13}C$ showed initial contributions of cDCE introduced with the inoculum. As is illustrated in Figure 2H,
235 the isotopic mass balance again confirms the near stoichiometric reduction of TCE to cDCE.

236 **Modeling Microbial Growth, TCE Hydrogenolysis, and Carbon Isotope Fractionation.** Using the
237 mathematical model described in eqs 2-10 we determined the microbiological growth parameters, that is
238 the maximum specific reaction rate of TCE hydrogenolysis, k, the Monod constant, K_M, and the
239 microbial growth yield, Y, pertinent to dehalorespiring organisms from simultaneously fitting all
240 measured data from experiments in the two- and three-phase system. As shown in Table 1, all
241 parameters agree reasonably well with previously reported values for *Sulfurospirillum multivorans*
242 (formerly referred to as *Dehalospirillum multivorans (33-35)*) and anaerobic mixed cultures *(23)*. Note
243 that k- and K_M-values calculated from the fitting of TCE concentration data to the model were assigned
244 as parameters describing the behavior of ^{12}C-TCE isotopologues (i.e., ^{12}k, $^{12}K_M$) while the ratio $^{13}k/^{13}K_M$
245 was obtained after fitting the model to measured $\delta^{13}C$ trends. TCE and cDCE concentrations and $\delta^{13}C$
246 values were modeled for all experimental system using the parameters listed in Table 1 including an
247 estimated tetradecane–aqueous phase mass-transfer coefficient κ_{TCE}^{org-aq}. A good agreement between
248 experimental data and model results was achieved (see data evaluation) except for the aqueous
249 concentration of TCE in the presence of tetradecane between 25 and 50 h (Figure 2B), which decreased
250 more rapidly than predicted by the model.
251

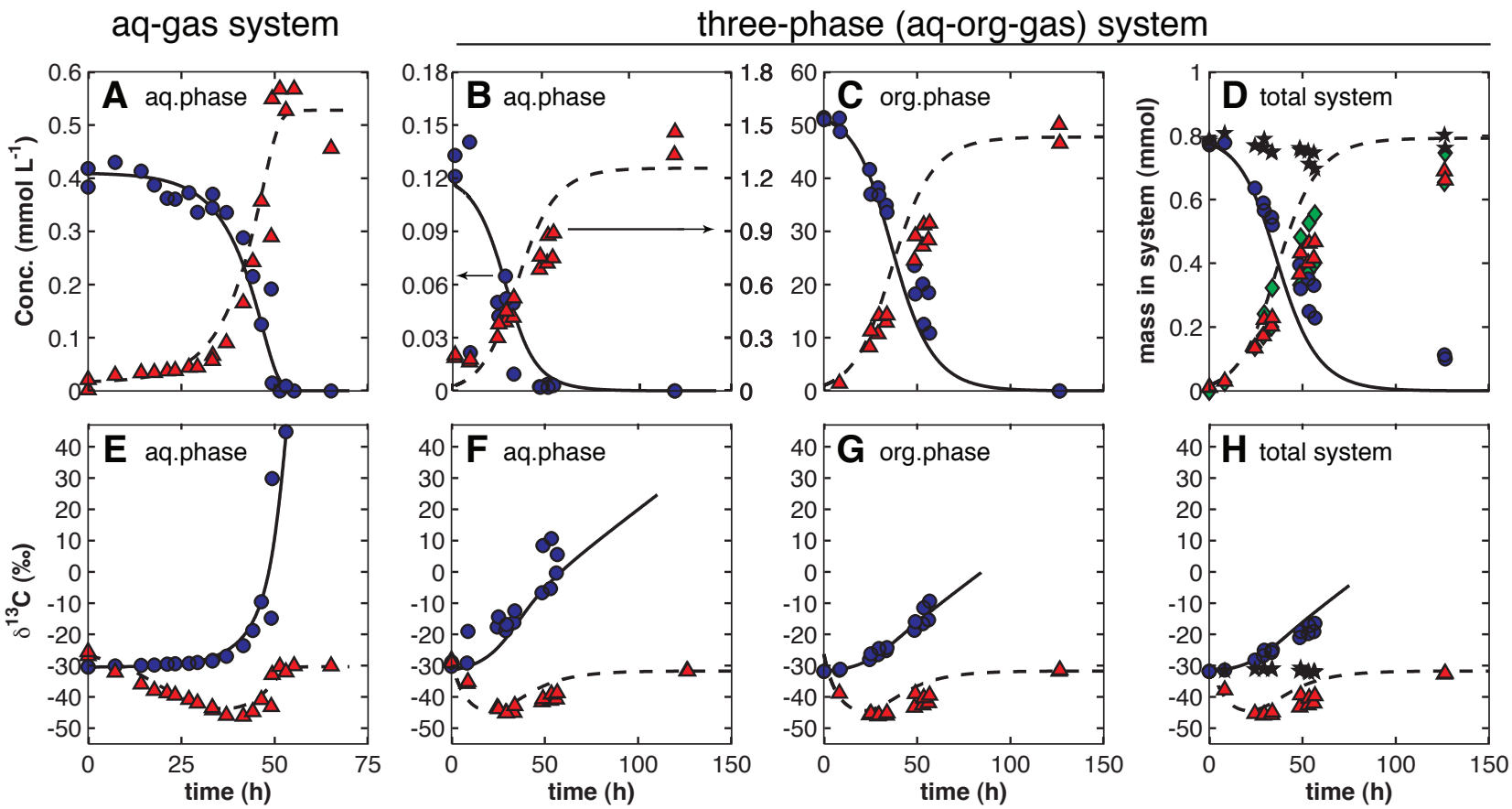

252

253 **Figure 2**: Changes in concentrations and carbon isotope signatures of TCE (blue circles and solid lines) and cDCE (red triangles and dashed lines) during
254 dehalogenation of TCE by *Sulfurospirillum sp*. Combined data from duplicate experiments are shown. Lines are simulations using the model described in the
255 methods section and parameters given in Table 1. Two-phase reference system; concentrations (panel A) and $\delta^{13}C$-values (panel E) of aqueous TCE and
256 cDCE. Three-phase system; concentrations (panels B, C) and $\delta^{13}C$-values (panels F, G) of TCE and cDCE in the aqueous and organic phases. Note that in
257 panel B, the concentration of TCE is given on the left-hand y-axis, while that of cDCE is shown on the right-hand y-axis as indicated with arrows. Panel D:
258 total TCE and cDCE in the system, sum of TCE and cDCE mass (stars) and mass of chloride released (green diamonds). Panel H: total TCE and cDCE
259 isotopic signatures in the system and isotopic mass balances (calculated from the sum of mass-weighted $\delta^{13}C$-values of TCE and cDCE in the organic and
260 aqueous phase, $\sum_{i=TCE,cDCE} \left(\delta^{13}C_i^{aq} \cdot m_i^{aq} + \delta^{13}C_i^{org} \cdot m_i^{org}\right) / m_i^{aq+org}$, stars). Measurement uncertainties in $\delta^{13}C$ are smaller than markers; errors in concentrations are
261 below 10% *(27)*.

Table 1: Maximum specific rates of reductive TCE dechlorination (^{12}k), microbial growth yield (Y), Monod-constants ($^{12}K_M$) and *n*-tetradecane – aqueous phase mass-transfer coefficients of TCE (κ_{TCE}^{org-aq}), as well as bulk carbon isotope enrichment factors, ε, for the reference system (ε_{ref}), ε observed in the presence of tetradecane (ε_{obs}), and ε calculated with the Rayleigh-equation ($\varepsilon_{obs,\,Rayleigh}$).

Data source	**Estimated parameters** [a]					**Model evaluation**	**Rayleigh evaluation**
	^{12}k (μmol cell^{-1} h^{-1})	Y (cells μmol^{-1})	$^{12}K_M$ (μmol L^{-1})	$\kappa_{org\text{-}aq}$ (cm·h^{-1})	ε_{ref} (‰)	ε_{obs} (‰)	$\varepsilon_{obs,Rayleigh}$ (‰)
All systems	6.1×10^{-9} (1.1) [b]	2.3×10^{7} (1.1) [b]	70 (1.2) [b]		-18.9±1.4 [b]		-
Two-phase system				-		-18.6 to -17.6	-18.8 ± 0.6 [b]
Three-phase system				35 (1.1) [b]		-18.4 to -5.9	-8.5 ± 1.1 [b]
Literature or reference system	(0.04 to 2.3)$\times10^{-9}$ [c,d,f]	(0.6 to 20)$\times10^{7}$ [d,e,f]	0.54 and 280 [d,g]	1.8±0.3 [h]			-12.8 to -18.5 [i]

a) Parameters were fit simultaneously for both replicates of the two- and three-phase system, except ε_{ref}, which was estimated exclusively in the two-phase system. b) Parentheses indicate uncertainty factor. Standard deviations of the estimated parameter values are obtained from division and multiplication by the uncertainty factor, respectively. Uncertainty of ε-values is ±1 standard deviation and r^2 were 0.99 and 0.95 in the two- and three-phase system, respectively. c) Reference *(33)* for *S. multivorans*. d) Reference *(23)*, modeling various dehalogenating

269 bacteria. e) Reference *(34)* for *S. multivorans*. f) Value converted for an assumed range of (mg cell-protein) cell^{-1} of 0.3x10^{-10} to 3.0x10^{-10} *(33,*

270 *34)*. g) Reference *(35)*. [h] This study (see experimental section). [i] Reference *(36-38)*

Quantification of Carbon Isotope Fractionation During Microbial TCE Reduction. The magnitude of isotope fractionation in the absence of transport limitations was calculated as reference fractionation factor, α_{ref} (eq. 9). Because the isotope fractionation factors are more commonly reported in bulk C isotope enrichment factors ε (in ‰), α-values were converted according to eq. 11.

$$\varepsilon_{ref} = (\alpha_{ref} - 1) \cdot 1000‰ \quad (11)$$

The fitted ε_{ref}-value pertinent to the ^{13}C enrichment of TCE in the two-phase system was -18.9±1.4‰ (Table 1). It is in the same order of magnitude as previously reported values for TCE hydrogenolysis by different *Sulfurospirillum* species determined in similar experimental systems, that is, ε-values were between -12.8±1.6 and -18.4±4.2‰ for *S. multivorans (36-38)* or -18.5±1.0‰ for *S. halorespirans (36)*. The ε_{ref}-value was insensitive to the gas-aqueous phase mass-transfer coefficient κ_{TCE}^{gas-aq} used in our model. Different fits with κ_{TCE}^{gas-aq}-values of 13 or 130 cm·h^{-1} caused ε_{ref} to change only insignificantly (i.e. ε_{ref} = -18.9±1.4 ‰ and -18.8±1.4‰, respectively). The identical ε–value of -18.8±0.6‰ was found when the aqueous phase $\delta^{13}C$ of TCE and its concentration were evaluated with a linearized form of the Rayleigh equation (eq. 1), which does not include effects of phase transfer. As show in Figure 3A (open circles), both approaches, eqs. 2-10 (solid line) and the Rayleigh model (dashed line), lead to the same result. This outcome confirms the applicability of our model and the chosen experimental conditions to study the C isotope fractionation of TCE hydrogenolysis in the absence of mass-transfer phenomena in the laboratory.

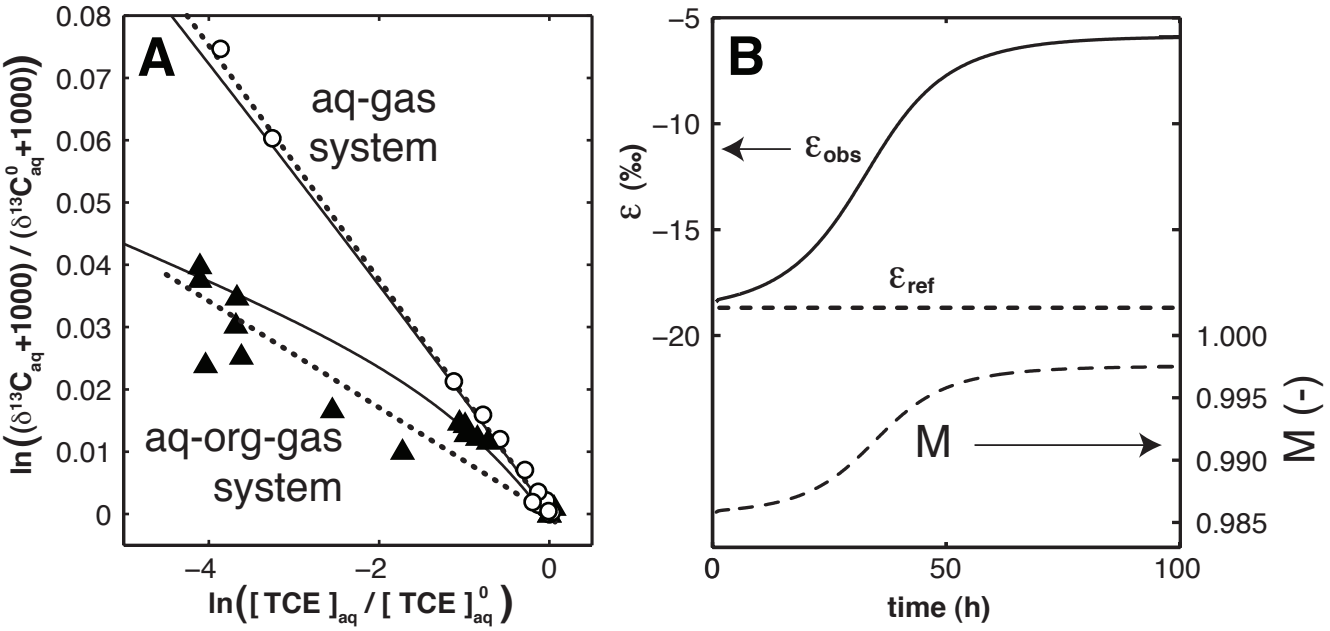

Figure 3: (A) Evaluation of $\delta^{13}C$ in TCE in the two-phase systems (aqueous and gaseous phase, open circles) and the three-phase system (aqueous-organic-gaseous phase, full triangles) according to a linearized form of eq. 1 (linearized Rayleigh equation). Solid lines represent data derived from the presented model (eqs. 2-11), dotted lines were obtained from a linear regression of the linearized form of Rayleigh eq 1. (B) Calculated trends of observed C isotope enrichment factor, ε_{obs}, for TCE (left y-axis) according to eqs 10-11 and ratio of inter-phase mass-transfer to microbial transformation rates (*M*, eq. 12, right y-axis). The reference isotope enrichment factor for the microbial TCE transformation, ε_{ref}, in the absence of mass-transfer limitations is shown as dotted line.

Effect of Mass Transfer on the Observed Carbon Isotope Fractionation in the Three-Phase System. In the presence of the tetradecane phase, trends of $\delta^{13}C$ for TCE and cDCE in the aqueous and organic phases were subject to mass-transfer limitations. This behavior became most obvious after 50 h when $\delta^{13}C$ for TCE increased more significantly in aqueous systems, that is in the absence of transport limitations (Figure 2E vs. 2F/2G). As is shown in Figure 3B, the calculated ^{13}C enrichment factors, ε_{obs}, which fit the $\delta^{13}C$ data in Figure 2F/G, corresponded only initially to ε_{ref} (i.e., -18.9±1.4‰), where TCE reduction proceeded without limitation by inter-phase mass transfer. The ε_{obs}-value decreased within 50

hours to -5.9‰ in a regime that was characterized by a limitation of TCE hydrogenolysis through the transport of TCE from the organic to the aqueous phase. This mass-transfer limited regime was observed after 50 hours concomitant with the rapid decrease of aqueous TCE concentration (Figures 2B and 2F). From abiotic reference experiments without *Sulfurospirillum sp*. we confirmed that this mass transfer is not accompanied with any significant isotope fractionation (Figure S1). The magnitude of the inter-phase mass-transfer velocity for assays containing *Sulfurospirillum sp*. (35±3 $cm \cdot h^{-1}$), however, was larger compared to κ_{TCE}^{org-aq} fit in reference experiments (1.8±0.3 $cm \cdot h^{-1}$). κ-values similar to those found in the reference experiments, that is between 1.0 and 1.8 $cm \cdot h^{-1}$, have been reported for the transfer of PCE or BTEX from non-aqueous phase liquids into aqueous solution *(21, 39)*. Beside the effect of differences in physical properties of cell suspensions and sterile medium, we hypothesize that the higher transfer velocity calculated for our experimental system containing *Sulfurospirillum* sp. reflects a situation, in which microorganisms might be localized preferably at the tetradecane-water interface rather than distributed homogeneously in the aqueous phase. These effects can lead to an apparent increase in mass-transfer and would be consistent with larger inter-phase mass-transfer velocities. This interpretation suggests that in a well-mixed system (no bacteria at the interface), the apparent masking of aqueous phase TCE isotope fractionation due to mass-transfer limitations might be even more pronounced.

We compared the relative contributions of TCE mass transfer *vs*. TCE reduction using the ratio of organic-aqueous mass-transfer rate and the rate of biodegradation, *M* (eq. 12).

$$M = \frac{\kappa_{TCE}^{org-aq} \cdot a_0^{aq} \cdot \left([TCE]_{aq}^{eq} - [TCE]_{aq} \right)}{{}^{12}r + {}^{13}r} \qquad (12)$$

The evolution of *M* with time is presented together with the trend of observed isotope enrichment factor, ε_{obs}, in Figure 3B. Throughout the entire experiment, *M* only varied between 0.985 and 0.997 indicating that minor changes of the ratio of transport *vs*. transformation rates by one percent can substantially alter the observable isotope fractionation, that is ε_{obs} decreased from -18.9‰ to -5.9‰

329 The consequences of an evaluation of TCE $\delta^{13}C$-values with a linearized Rayleigh model are shown in
330 Figure 3A. As pointed out recently *(18, 22)*, mass-transport based kinetic limitations result in typical
331 deviations from the linear correlation usually reported for $\ln[(\delta^{13}C + 1000‰)/(\delta^{13}C_0 + 1000‰)]$ *vs*. $\ln$
332 (C/C_0). Such a linear fit of $\delta^{13}C$ for TCE to a linearized eq. 1 gives rise to an "average" ε_{obs} of -
333 8.5±1.1‰, which underestimated the initial fractionation while overestimating it at later stages of the
334 reaction. This interpretation qualitatively agrees with the masking of hydrogen isotope fractionation
335 observed during the aerobic toluene oxidation by *Pseudomonas putida* in laboratory batch reactors *(18)*.
336 Kampara et al. *(18)* found that under non-growth conditions, lower substrate concentrations were
337 indicative of limited bioavailability. The kinetics of the non-isotopic substrate mass-transfer to the
338 location of the enzyme and/or its active site was shown to decrease the magnitude of hydrogen isotope
339 fractionation. Given the concentration range of aqueous TCE investigated in this work, however, we do
340 not think that the TCE hydrogenolysis kinetics were limited by bioavailability constraints. As is shown
341 in Figure 3A for the two-phase system, no deviations from the linearized Rayleigh equation were found
342 while aqueous TCE concentration decreased from 400 to 8 μmol·L^{-1}, that is to a regime of $[TCE_{aq}]/K_M$
343 below 1 (K_M according to Table 1), which was suggested to be characteristic for a mass-transfer limited
344 contaminant biodegradation *(18)*. Therefore, we attribute the observed masking effect on ε_{obs} to the
345 kinetics of inter-phase TCE mass transfer. This interpretation nevertheless does not rule out additional
346 modulation of isotopic effects during hydrogenolysis at $[TCE_{aq}]/K_M$ ratios <1 which were not accessible
347 to isotope ratio measurements in our experiments.

348 **Implications for field applications.** Dissolution rates of non-aqueous phase liquids containing
349 chloroethenes are highly variable and depend on a number of factors pertinent to the contaminated
350 subsurface (i.e., NAPL architecture, groundwater velocity, biomass distribution, etc.) and the
351 composition of the organic contamination *(19-21)*. For flow regimes, under which dissolution kinetics
352 are not controlled by advective-diffusive transport and for which the evaluation of isotope fractionation
353 of chloroethenes in the field is usually reported *(4, 6, 8, 40)*, our results have important implications.

354 Our study shows that stable isotope fractionation associated with contaminant (bio-)degradation not
355 only can be modulated by bioavailability constraints but also due to inter-phase mass-transfer processes
356 that occur during the dissolution of contaminants from non-aqueous phase liquids. The tetradecane
357 phase used here to mimic a NAPL in the laboratory represents situations, where TCE has been spilled
358 together with hydrocarbon fuels *(8, 41)*. Under such conditions, an assessment of contaminant
359 transformation on the basis of CSIA is hampered as ε-values likely vary within the proposed range.
360 Assuming a shift of measured $\delta^{13}C$-values between two sampling locations in a contaminated aquifer by
361 ±1‰ - a precision, which can commonly be resolved with standard CSIA methods *(28, 42)* - estimates
362 of the fraction of transformed contaminant may vary between 5% and 16% depending on the ε-value
363 used for the assessment (Figure 3B).
364 Evaluation of TCE isotope fractionation at field sites contaminated with dense non-aqueous phase
365 liquids (DNAPLs) of TCE can be more difficult. In contrast to the model system studied here, both TCE
366 concentration and its $\delta^{13}C$-values in the DNAPL are not expected to vary unless the DNAPL is largely
367 dissolved. While inter-phase mass transfer velocities from the pure phase TCE to the aqueous phase are
368 similar to the system investigated here (see above), the pure phase contains much more TCE so that
369 isotopic shifts of TCE within the NAPL would develop much slower. Also, mass fluxes of TCE from
370 the NAPL to the water will be considerably larger than from a mixed NAPL. The latter should give rise
371 to less masking of the TCE isotope fractionation from biodegradation given that growth of
372 dehalorespiring microorganism is often limited through competition with other hydrogenotrophic
373 bacteria for hydrogen *(23)*. Increased TCE dissolution rates, however, can result in steady-state aqueous
374 TCE concentrations that reflect the isotopic composition within the DNAPL because TCE dissolution
375 causes only very minor isotope fractionation *(40)*. Thus, in spite of ongoing biodegradation and
376 concomitant C isotope fractionation, aqueous TCE ^{13}C signatures might not show significant ^{13}C
377 enrichment owing to DNAPL dissolution. Such situations have been reported for TCE contaminations in
378 the field *(6)* but ongoing biodegradation was nevertheless identified via isotope enrichment trends

observed in the hydrogenolysis products. Further study is necessary to delineate the DNAPL dissolution regimes that may compromise the application of CSIA.

Acknowledgments

This project was funded by the Swiss Federal Office for the Environment. We are thankful to Emmanuelle Rohrbach from EPFL Lausanne for providing support in microbial cultivation. Susanne Schuepbach and Frederik Hammes are acknowledged for experimental assistance. We thank Daniel Hunkeler for helpful comments on an early version of the manuscript.

Supporting Information Available

Detailed analytical methods, details on sterile mass-transfer experiments and concentration and isotopic mass balance of the three-phase system as well as MATLAB codes of the presented model are provided in Supporting Information.

Literature Cited

1. Holliger, C.; Regeard, C.; Diekert, G. Dehalogenation by anaerobic bacteria. In *Dehalogenation - Microbial Processes and Environmental Applications*, Haeggblom, M. M.; Bossert, I. D., Eds. Kluwer Academic Publishers: 2003; pp 115-157.

2. Meckenstock, R.U.; Morasch, B.; Griebler, C.; Richnow, H.H. Stable isotope fractionation analysis as a tool to monitor biodegradation in contaminated aquifers. *J. Contam. Hydrol.* **2004,** *75*, 215-255.

3. Schmidt, T.C.; Zwank, L.; Elsner, M.; Berg, M.; Meckenstock, R.U.; Haderlein, S.B. Compound-specific stable isotope analysis of organic contaminants in natural environments: a critical review of the state of the art, prospects, and future challenges. *Anal. Bioanal. Chem.* **2004,** *378*, 283-300.

4. Sherwood Lollar, B.; Slater, G.F.; Sleep, B.; Witt, M.; Klecka, G.M.; Harkness, M.; Spivack, J. Stable carbon isotope evidence for intrinsic bioremediation of tetrachloroethene and trichloroethene at area 6, Dover Air Force Base. *Environ. Sci. Technol.* **2001,** *35*, 261-269.

5. Vieth, A.; Muller, J.; Strauch, G.; Kastner, M.; Gehre, M.; Meckenstock, R.U.; Richnow, H.H. In-situ biodegradation of tetrachloroethene and trichloroethene in contaminated aquifers monitored by stable isotope fractionation. *Isot. Environ. Health Stud.* **2003,** *39*, 113-124.

6. Chartrand, M.M.G.; Morrill, P.L.; Lacrampe-Couloume, G.; Sherwood Lollar, B. Stable isotope evidence for biodegradation of chlorinated ethenes at a fractured bedrock site. *Environ. Sci. Technol.* **2005,** *39*, 4848-4856.

7. Hirschorn, S.K.; Grostern, A.; Lacrampe-Couloume, G.; Elizabeth, A.E.B.; MacKinnon, L.; Repta, C.; Major, D.W.; Sherwood Lollar, B. Quantification of biotransformation of chlorinated hydrocarbons in a biostimulation study: Added value via stable carbon isotope analysis. *J. Contam. Hydrol.* **2007,** *94*, 249-260.

8. Morrill, P.L.; Lacrampe-Couloume, G.; Slater, G.F.; Sleep, B.E.; Edwards, E.A.; McMaster, M.L.; Major, D.W.; Sherwood Lollar, B. Quantifying chlorinated ethene degradation during reductive dechlorination at Kelly AFB using stable carbon isotopes. *J. Contam. Hydrol.* **2005,** *76*, 279-293.

9. Abe, Y.; Hunkeler, D. Does the Rayleigh equation apply to evaluate field isotope data in contaminant hydrogeology? *Environ. Sci. Technol.* **2006,** *40*, 1588-1596.

10. Cichocka, D.; Imfeld, G.; Richnow, H.H.; Nijenhuis, I. Variability in microbial carbon isotope fractionation of tetra- and trichloroethene upon reductive dechlorination. *Chemosphere* **2008,** *71*, 639-648.

11. Abe, Y.; Aravena, R.; Zopfi, J.; Shouakar-Stash, O.; Cox, E.; Roberts, J.D.; Hunkeler, D. Carbon and chlorine isotope fractionation during aerobic oxidation and reductive dechlorination of vinyl chloride and cis-1,2-dichloroethene. *Environ. Sci. Technol.* **2009,** *43*, 101-107.

12. Slater, G.F.; Sherwood Lollar, B.; Sleep, B.E.; Edwards, E.A. Variability in carbon isotopic fractionation during biodegradation of chlorinated ethenes: Implications for field applications. *Environ. Sci. Technol.* **2001,** *35*, 901-907.

13. Bloom, Y.; Aravena, R.; Hunkeler, D.; Edwards, E.; Frape, S.K. Carbon isotope fractionation during microbial dechlorination of trichloroethene, cis-1,2-dichloroethene, and vinyl chloride: Implications for assessment of natural attenuation. *Environ. Sci. Technol.* **2000,** *34*, 2768-2772.

14. Zwank, L.; Berg, M.; Elsner, M.; Schmidt, T.C.; Schwarzenbach, R.P.; Haderlein, S.B. New evaluation scheme for two-dimensional isotope analysis to decipher biodegradation processes: Application to groundwater contamination by MTBE. *Environ. Sci. Technol.* **2005,** *39*, 1018-1029.

15. Hofstetter, T.B.; Reddy, C.M.; Heraty, L.J.; Berg, M.; Sturchio, N.C. Carbon and chlorine isotope effects during abiotic reductive dechlorination of polychlorinated ethanes. *Environ. Sci. Technol.* **2007,** *41*, 4662-4668.

16. Hofstetter, T.B.; Spain, J.C.; Nishino, S.F.; Bolotin, J.; Schwarzenbach, R.P. Identifying competing aerobic nitrobenzene biodegradation pathways using compound-specific isotope analysis. *Environ. Sci. Technol.* **2008,** *42*, 4764-4770.

17. Shouakar-Stash, O.; Drimmie, R.J.; Zhang, M.; Frape, S.K. Compound-specific chlorine isotope ratios of TCE, PCE and DCE isomers by direct injection using CF-IRMS. *Appl. Geochem.* **2006,** *21*, 766-781.

18. Kampara, M.; Thullner, M.; Richnow, H.H.; Harms, H.; Wick, L.Y. Impact of bioavailability restrictions on microbially induced stable isotope fractionation. 2. Experimental evidence. *Environ. Sci. Technol.* **2008,** *42*, 6552-6558.

19. Sleep, B.E.; Seepersad, D.J.; Mo, K.; Heidorn, C.M.; Hrapovic, L., *et al*. Biological enhancement of tetrachloroethene dissolution and associated microbial community changes. *Environ. Sci. Technol.* **2006,** *40*, 3623-3633.

20. Powers, S.E.; Abriola, L.M.; Weber, W.J. An experimental investigation of nonaqueous phase liquid dissolution in saturated subsurface systems - Steady-state mass transfer rates. *Water Resour. Res.* **1992,** *28*, 2691-2705.

21. Amos, B.K.; Christ, J.A.; Abriola, L.M.; Pennell, K.D.; Loffler, F.E. Experimental evaluation and mathematical modeling of microbially enhanced tetrachloroethene (PCE) dissolution. *Environ. Sci. Technol.* **2007,** *41*, 963-970.

22. Thullner, M.; Kampara, M.; Richnow, H.H.; Harms, H.; Wick, L.Y. Impact of bioavailability restrictions on microbially induced stable isotope fractionation. 1. Theoretical calculation. *Environ. Sci. Technol.* **2008,** *42*, 6544-6551.

23. Fennell, D.E.; Gossett, J.M. Modeling the production of and competition for hydrogen in a dechlorinating culture. *Environ. Sci. Technol.* **1998,** *32*, 2450-2460.

24. van Breukelen, B.M.; Hunkeler, D.; Volkering, F. Quantification of sequential chlorinated ethene degradation by use of a reactive transport model incorporating isotope fractionation. *Environ. Sci. Technol.* **2005,** *39*, 4189-4197.

25. Becker, J.G. A modeling study and Implications of competition between *Dehalococcoides ethenogenes* and other tetrachloroethene-respiring bacteria. *Environ. Sci. Technol.* **2006,** *40*, 4473-4480.

26. Holliger, C.; Hahn, D.; Harmsen, H.; Ludwig, W.; Schumacher, W.; Tindall, B.; Vazquez, F.; Weiss, N.; Zehnder, A.J.B. *Dehalobacter restrictus* gen. nov. and sp. nov., a strictly anaerobic bacterium that reductively dechlorinates tetra- and trichloroethene in an anaerobic respiration. *Arch. Microbiol.* **1998,** *169*, 313-321.

27. Aeppli, C.; Berg, M.; Hofstetter, T.B.; Kipfer, R.; Schwarzenbach, R.P. Simultaneous quantification of polar and non-polar volatile organic compounds in water samples by direct aqueous injection-gas chromatography/mass spectrometry. *Journal of Chromatography A* **2008,** *1181*, 116-124.

28. Zwank, L.; Berg, M.; Schmidt, T.C.; Haderlein, S.B. Compound-specific carbon isotope analysis of volatile organic compounds in the low-microgram per liter range. *Analytical Chemistry* **2003,** *75*, 5575-5583.

29. Hammes, F.A.; Egli, T. New method for assimilable organic carbon determination using flow-cytometric enumeration and a natural microbial consortium as inoculum. *Environ. Sci. Technol.* **2005,** *39*, 3289-3294.

30. Powers, S.E.; Abriola, L.M.; Dunkin, J.S.; Weber, W.J. Phenomenological models for transient NAPL-water mass-transfer processes. *J. Contam. Hydrol.* **1994,** *16*, 1-33.

31. Cleland, W.W. Enzyme Mechanisms from Isotope Effects. In *Isotope Effects in Chemistry and Biology*, Kohen, A.; Limbach, H., Eds. CRC Press / Taylor & Francis: New York, 2006; pp 915-930.

32. Schwarzenbach, R.P.; Gschwend, P.M.; Imboden, D.M. *Environmental Organic Chemistry*. 2nd ed.; John Wiley & Sons: New York, 2003; p 1311.

33. Neumann, A.; Scholz-Muramatsu, H.; Diekert, G. Tetrachloroethene metabolsim of *Dehalospirillum multivorans*. *Arch. Microbiol.* **1994,** *162*, 295-301.

34. Scholz-Muramatsu, H.; Neumann, A.; Messmer, M.; Moore, E.; Diekert, G. Isolation and characterization of *dehalospirillum multivorans* gen. nov., sp. nov., A tetrachloroethene-utilizing, strictly anaerobic bacterium. *Arch. Microbiol.* **1995,** *163*, 48-56.

35. Neumann, A.; Wohlfarth, G.; Diekert, G. Purification and characterization of tetrachloroethene reductive dehalogenase from *Dehalospirillum multivorans*. *J. Biol. Chem.* **1996,** *271*, 16515-16519.

491 36. Cichocka, D.; Siegert, M.; Imfeld, G.; Andert, J.; Beck, K.; Diekert, G.; Richnow, H.H.;
492 Nijenhuis, I. Factors controlling the carbon isotope fractionation of tetra- and trichloroethene during
493 reductive dechlorination by *Sulfurospirillum* ssp and *Desulfitobacterium* sp strain PCE-S. *FEMS*
494 *Microbiol. Ecol.* **2007,** *62*, 98-107.

495 37. Lee, P.K.H.; Conrad, M.E.; Alvarez-Cohen, L. Stable carbon isotope fractionation of
496 chloroethenes by dehalorespiring isolates. *Environ. Sci. Technol.* **2007,** *41*, 4277-4285.

497 38. Liang, X.; Dong, Y.; Kuder, T.; Krumholz, L.R.; Philp, R.P.; Butler, E.C. Distinguishing abiotic
498 and biotic transformation of tetrachloroethylene and trichloroethylene by stable carbon isotope
499 fractionation. *Environ. Sci. Technol.* **2007,** *41*, 7094-7100.

500 39. Schluep, M.; Imboden, D.M.; Galli, R.; Zeyer, J. Mechanisms affecting the dissolution of
501 nonaqueous phase liquids into the aqueous phase in slow stirring batch systems. *Environ. Toxicol.*
502 *Chem.* **2001,** *20*, 459-466.

503 40. Hunkeler, D.; Chollet, N.; Pittet, X.; Aravena, R.; Cherry, J.A.; Parker, B.L. Effect of source
504 variability and transport processes on carbon isotope ratios of TCE and PCE in two sandy aquifers. *J.*
505 *Contam. Hydrol.* **2004,** *74*, 265-282.

506 41. VanStone, N.; Przepiora, A.; Vogan, J.; Lacrampe-Couloume, G.; Powers, B.; Perez, E.;
507 Mabury, S.; Sherwood Lollar, B. Monitoring trichloroethene remediation at an iron permeable reactive
508 barrier using stable carbon isotopic analysis. *J. Contam. Hydrol.* **2005,** *78*, 313-325.

509 42. Sherwood Lollar, B.; Hirschorn, S.K.; Chartrand, M.M.G.; Lacrampe-Couloume, G. An
510 approach for assessing total instrumental uncertainty in compound-specific carbon isotope analysis:
511 Implications for environmental remediation studies. *Anal. Chem.* **2007,** *79*, 3469-3475.

512

513 **Brief**

514 The kinetics of trichloroethene inter-phase mass transfer between tetradecane and water modulate the
515 observable ^{13}C enrichment pertinent to trichloroethene dehydrochlorination by *Sulfurospirillum sp.* in
516 laboratory batch systems.

517

518